A Two-Stage Stochastic Unit Commitment Model for Wind-integrated Power Systems Flexibility Assessment

Rodrigo Mena
Department of Industrial Engineering
Universidad Técnica
Federico Santa María
Santiago, Chile
rodrigo.mena@usm.cl

Cristóbal Catalán
Department of Industrial Engineering
Universidad Técnica
Federico Santa María
Santiago, Chile
cristobal.catalan@sansano.usm.cl

Pablo Viveros
Department of Industrial Engineering
Universidad Técnica
Federico Santa María
Valparaíso, Chile
pablo.viveros@usm.cl

Enrico Zio
Centre for research on Risks and Crises
MINES ParisTech
Sophia Antípolis, France
Energy Department
Politecnico di Milano
Milano, Italia
enrico.zio@polimi.it

2022 17th International Conference on Probabilistic Methods Applied to Power Systems (PMAPS) | 978-1-6654-1211-7/22/$31.00 ©2022 IEEE | DOI: 10.1109/PMAPS53380.2022.9810585

***Abstract*—Decision making regarding the operation of renewable-integrated power systems have become increasingly complex in view of the need for flexibility, i.e., the ability to accommodate time-dependent variability arising from the interactions between uncertainties in the demand and renewable power sources. In this paper, a two-stage stochastic unit commitment program is proposed to determine cost-effective on/off schedules for a wind-integrated power system. Uncertainties in the aggregated load and wind power generation are considered to generate random operating scenarios. Generation-side flexibility metrics are introduced to trace and analyze events of energy not supplied and/or wind power curtailment. An application of the proposed optimization program is conducted for a modification of the New England IEEE 39-Bus test system. The results show the usefulness of the model for generation scheduling and providing valuable insights regarding the design of operational strategies for efficient use of wind power.**

***Index Terms*—Power systems, wind energy, flexibility, unit commitment, stochastic programming.**

I. Introduction

During the last decades, most of the nations committed to sustainability have been implementing various renewable energy policies to promote the integration of significant shares of renewables into power systems [1]. The International Energy Agency reports in [2] that the global renewable generation capacity is on the rise, with an important contribution of wind power technologies. However, the integration of high shares of wind energy into existing power systems poses increased complexities regarding decisions on infrastructure planning and operations. These complexities are a consequence of the inherent variable (uncertain) nature of wind speed and, therefore, of wind power, that interacts with other sources of uncertainty, such as the load, to generate a highly dynamic, time-dependent and uncertain operational environment [3].

From an operational perspective, the interaction of uncertain wind power and loads translates into uncertain net-load profiles. Then, to accommodate high rates of variable wind power requires a dispatchable generation fleet that provides enough flexibility to meet the net-load ramp requirements without compromising the reliability of power supply [4]. From a risk analysis perspective, it is of interest to identify the combination of factors, including net-load variability and (in)sufficiency of flexibility, and decisions leading to negative operational outcomes with respect to the planning objectives, such as energy not supplied or excessive wind power curtailment [5].

Enabling the above mentioned type of analysis entails the modeling of the operation of the power system to assess diverse operational attributes of interest and, in particular, flexibility. Various research works have resorted to mathematical programming to this end, through variants of the economic dispatch (ED) [6], [7], optimal power flow (OPF) [4], and unit commitment (UC) [3] models; and correspondingly proposing different metrics to evaluate requirements, availability and (in)sufficiency of flexibility. The UC model raises particular interest since it allows a proper modeling of the sequentially time–dependent capabilities of cycling and ramping of conventional generation units that condition the deployment of power over time and, therefore, the extent of available flexibility.

In this work, we address the problem of modeling the

This work was supported by ANID (ANID/FONDECYT/11190269)

operation of a wind-integrated power system accounting for uncertainty in wind power generation and the aggregated demand of the system. For this, we propose a two-stage stochastic unit commitment model that embeds a sequential Montecarlo Simulation (MCS) to sample different realizations of the sources of uncertainty. The model is formulated as a mixed integer linear program (MILP) and aims at finding an on/off schedule that minimizes the expected value of the total operating cost. Then, an *a posteriori* flexibility assessment is performed on the cost-optimal on/off schedule. This is done by introducing flexibility indicators into the modeling framework, to trace the implications of the scheduling decisions on the (in)suficiency of flexibility provided by the dispatchable generation fleet of the system, and the associated impacts for extreme scenarios of wind power curtailment.

II. Problem Formulation

The power system is modeled as a graph composed by a set of nodes $\mathcal{N}$, accounting for the locations of loads and generation units, and a set of edges $\mathcal{L}$ representing transmission lines that connect the nodes. Generation units are grouped into two sets, $\mathcal{G}$ and $\mathcal{W}$, denoting conventional generation units and wind power units, respectively.

For the construction of an optimal on/off schedule throughout a horizon $\mathcal{T}$, the two-stage stochastic UC model considers as sources of uncertainty the aggregated demand of the system and the nodal wind speeds. The realization of different scenarios ξ of these parameters, explored by means of MCS, are represented by the set Ω.

A. Uncertain parameters

1) Aggregated demand: The aggregated demand of the system D_t (MW), over a given time period $t \in \mathcal{T}$ (e.g. one hour), is considered as normally distributed with mean μ_t and variance σ_t^2 [8]. Then, realizations of the aggregated demand profiles $\{D_{t,\xi}\}_{t=1,\dots,|T|}$ with $\xi \in \Omega$ are sampled from the normal distributions corresponding to each period $t \in \mathcal{T}$.

The nodal demand profiles for each scenario $\xi \in \Omega$, $\{D_{i,t,\xi}\}_{t=1,\dots,|T|}$, are built by weighing down the aggregated profile by a nodal factor $p_i, \forall i \in \mathcal{N}$, with $\sum_{i\in\mathcal{N}} p_i = 1$.

2) Wind speed: At nodes $i \in \mathcal{N}$ where wind power units are located, discrete wind speed time series $\{ws_{i,t,\xi}\}_{t=1,..,|\mathcal{T}|}$ are sampled by means of Seasonal Autoregressive Integrated Moving Average (SARIMA) models [9] for each scenario $\xi \in \Omega$. Each sampled wind speed time series is given in input to a wind energy conversion model $c^{\mathrm{W}}(ws_{i,t,\xi})$ [10], as in (1), to determine the available wind power P^{W} (MW) for a number of N_i^{W} wind turbines located at node $i \in \mathcal{N}$, as presented in (2),

$$c^{\mathrm{W}}(ws_{i,t,\xi}) = \begin{cases} 0 & 0 < ws_{i,t,\xi} < U^{\mathrm{in}} \\ \dfrac{ws_{i,t,\xi} - U^{\mathrm{in}}}{U^{\mathrm{R}} - U^{\mathrm{in}}} & U^{\mathrm{in}} \le ws_{i,t,\xi} < U^{\mathrm{R}} \\ 1 & U^{\mathrm{R}} \le ws_{i,t,\xi} < U^{\mathrm{out}} \\ 0 & \text{otherwise} \end{cases} \quad (1)$$

$$P^{W}(ws_{i,t,\xi}) = N_i^{\mathrm{W}} P^{\mathrm{R}} c^{\mathrm{W}}(ws_{i,t,\xi}) \quad (2)$$

where P^{R} (MW) is the rated power of the wind turbine, and U^{in}, U^{R} and U^{out} (m/s) are the cut-in, rated and cut-out wind speeds, respectively.

B. Objective function

The objective function (3) to be minimized corresponds to the expected value of total cost quantity, given a set of equiprobable scenarios Ω with probability $\mathbb{P}^{\xi}$,

$$\begin{aligned} \min_X \quad & \mathbf{E}(C_\xi^{\mathrm{T}}) = \mathbb{P}^{\xi} \sum_{\xi\in\Omega} \Bigg\{ \sum_{t\in\mathcal{T}} \sum_{g\in\mathcal{G}\cup\mathcal{W}} C_g^{\mathrm{OM}} P_{g,t,\xi} \Delta t + \\ & \sum_{t\in\mathcal{T}} \sum_{g\in\mathcal{G}} x_{g,t} C_g^{\mathrm{F}} \Delta t + \sum_{t\in\mathcal{T}} \sum_{g\in\mathcal{G}} (u_{g,t} C_g^{\mathrm{SU}} + v_{g,t} C_g^{\mathrm{SD}}) + \\ & \sum_{t\in\mathcal{T}} \sum_{g\in\mathcal{G}} P_{g,t,\xi} \Delta t H_g \mu_g^{\mathrm{f}} C^{\mathrm{CO_2}} + \sum_{t\in\mathcal{T}} \sum_{i\in\mathcal{N}} LS_{i,t,\xi} \Delta t C_i^{\mathrm{ENS}} \\ & \sum_{\substack{t\in\mathcal{T},\\ t\ge 2}} \sum_{g\in\mathcal{G}} C_g^{\mathrm{R}} (\Delta P^{\mathrm{U}}_{g,(t-1,t),\xi} - \Delta P^{\mathrm{D}}_{g,(t-1,t),\xi}) \Bigg\} \end{aligned} \quad (3)$$

where $P_{g,t,\xi} \ge 0$ are decision variables representing the power in (MW) produced by generator g at period t for the scenario ξ, and C_g^{OM} is the variable O&M generation cost in (US$/MWh). $x_{g,t} \in \{0,1\}$ are binary decisions variables that take the value 1 when the generation unit g is on at period t and takes the value 0 otherwise. C_g^{F} is the fixed cost of keeping the generation unit g on for a period of time, measured in (US$/h). $u_{g,t}, v_{g,t} \in \{0,1\}$ are binary decision variables that take the value 1 when generation unit g is started up or shut down at period t, respectively. C_g^{SU} and C_g^{SD} are the start-up and shut down costs in (US$). H_g and μ_g^{f} are, respectively, the full load heat rate in (MMBtu/MWh) and the carbon intensity in (tCO_2/MMBtu) associated to the fuel used by generator g. $C^{\mathrm{CO_2}}$ is the carbon cost in (US$/$tCO_2$). $LS_{i,t,\xi} \ge 0$ are decision variables representing the load shedding in (MW) at node i at period t for the scenario ξ, and C_i^{ENS} is the penalty cost for the energy not supplied at node i, measured in (US$/MWh). $\Delta P^{\mathrm{U}}_{g,(t-1,t),\xi} \ge 0$ and $\Delta P^{\mathrm{D}}_{g,(t-1,t),\xi} \le 0$ are decision variables representing the positive and negative power output ramps provided by generator g from period $t-1$ to t for the scenario ξ and C_g^{R} in (US$/$\Delta$MW) is the ramping cost of generator g.

C. Commitment constraints

The first stage of the stochastic UC model considers commitment decisions, restricted by the conditions below:

$$u_{g,t} + v_{g,t} \le 1, \qquad \forall g \in \mathcal{G}, t \in \mathcal{T} \quad (4)$$

$$x_{g,t} - x_{g,t-1} = u_{g,t} - v_{g,t}, \forall g \in \mathcal{G}, t \in \mathcal{T}, t \ge 2 \quad (5)$$

$$x_{g,1} = u_{g,1}, \qquad \forall g \in \mathcal{G} \quad (6)$$

$$t_g^{\mathrm{U}} u_{g,t} \le \sum_{\tau=t}^{t+t_g^{\mathrm{U}}-1} x_{g,\tau}, \qquad \forall g \in \mathcal{G}, t \in \mathcal{T}, \; t \le |T| - t_g^{\mathrm{U}} \quad (7)$$

$$(|T|-t+1)\,u_{g,t} \le \sum_{\tau=t}^{|T|} x_{g,\tau}, \qquad \begin{array}{r}\forall g\in\mathcal{G}, t\in\mathcal{T},\\ t\ge |T|-t_g^{\mathrm{U}}+1\end{array} \quad (8)$$

$$t_g^{\mathrm{D}} v_{g,t} \le \sum_{\tau=t}^{t+t_g^{\mathrm{D}}-1}(1-x_{g,\tau}), \qquad \begin{array}{r}\forall g\in\mathcal{G}, t\in\mathcal{T},\\ t\le |T|-t_g^{\mathrm{D}}\end{array} \quad (9)$$

$$(|T|-t+1)\,v_{g,t} \le \sum_{\tau=t}^{|T|}(1-x_{g,\tau}), \qquad \begin{array}{r}\forall g\in\mathcal{G}, t\in\mathcal{T},\\ t\ge |T|-t_g^{\mathrm{D}}+1\end{array} \quad (10)$$

Constraints set (4) impose that a generation unit g can either be started up or shut down at period t, but not both. Constraint sets (5) and (6) relate in time the status variables $x_{g,t}$ with the start up and shut down decisions, $u_{g,t}$ and $v_{g,t}$, respectively. Constraints sets (7),(8), (9), (10), force generation unit g to stay on or to cool off for at least t_g^{U} and t_g^{D} periods, respectively, before changing status again.

D. Dispatching constraints

The second stage of the model, in which uncertainty is introduced, regards power dispatching decisions. The corresponding constraints are based on the DC power flow approximation [11] and are declared below:

$$\begin{array}{l}\sum_{g\in\mathcal{G}_i\cup\mathcal{W}_i} P_{g,t,\xi} + \sum_{(j,i)\in\mathcal{L}} B_{(j,i)}\Delta\theta_{(j,i),t,\xi} - \\ \sum_{(i,j)\in\mathcal{L}} B_{(i,j)}\Delta\theta_{(i,j),t,\xi} + LS_{i,t,\xi} = D_{i,t,\xi},\end{array} \qquad \begin{array}{r}\forall i\in\mathcal{N}, t\in\mathcal{T},\\ \xi\in\Omega\end{array} \quad (11)$$

$$P_g^{\min} x_{g,t} \le P_{g,t,\xi}, \qquad \forall g\in\mathcal{G}, t\in\mathcal{T}, \xi\in\Omega \quad (12)$$

$$P_{g,t,\xi} \le P_g^{\max} x_{g,t} - r_{g,t,\xi}, \qquad \forall g\in\mathcal{G}, t\in\mathcal{T}, \xi\in\Omega \quad (13)$$

$$\sum_{g\in\mathcal{G}} r_{g,t,\xi} \ge r_t^{\min} \qquad \forall t\in\mathcal{T}, \xi\in\Omega \quad (14)$$

$$P_{g,t,\xi} + PC^{\mathrm{W}}_{g,t,\xi} = P^{\mathrm{W}}(ws_{i,t,\xi}), \qquad \begin{array}{r}\forall i\in\mathcal{N}, g\in\mathcal{W}_i,\\ t\in\mathcal{T}, \xi\in\Omega\end{array} \quad (15)$$

$$B_{(i,j)}\Delta\theta_{(i,j),t,\xi} \le P^{\mathrm{R}}_{(i,j)}, \qquad \forall (i,j)\in\mathcal{L}, t\in\mathcal{T}, \xi\in\Omega \quad (16)$$

$$-B_{(i,j)}\Delta\theta_{(i,j),t,\xi} \le P^{\mathrm{R}}_{(i,j)}, \qquad \forall (i,j)\in\mathcal{L}, t\in\mathcal{T}, \xi\in\Omega \quad (17)$$

$$P_{g,t,\xi} - P_{g,t-1,\xi} \le r_g^{\mathrm{U}} P_g^{\max} x_{g,t-1} + r_g^{\mathrm{SU}} u_{g,t}, \qquad \begin{array}{r}\forall g\in\mathcal{G}, t\in\mathcal{T},\\ t\ge 2, \xi\in\Omega\end{array} \quad (18)$$

$$P_{g,t-1,\xi} - P_{g,t,\xi} \le r_g^{\mathrm{D}} P_g^{\max} x_{g,t} + r_g^{\mathrm{SD}} v_{g,t}, \qquad \begin{array}{r}\forall g\in\mathcal{G}, t\in\mathcal{T},\\ t\ge 2, \xi\in\Omega\end{array} \quad (19)$$

$$P_{g,t,\xi} - P_{g,t-1,\xi} \le \Delta P^{\mathrm{U}}_{g,t,\xi}, \qquad \begin{array}{r}\forall g\in\mathcal{G}, t\in\mathcal{T},\\ t\ge 2, \xi\in\Omega\end{array} \quad (20)$$

$$P_{g,t-1,\xi} - P_{g,t,\xi} \le -\Delta P^{\mathrm{D}}_{g,t,\xi}, \qquad \begin{array}{r}\forall g\in\mathcal{G}, t\in\mathcal{T},\\ t\ge 2, \xi\in\Omega\end{array} \quad (21)$$

Constraints set (11) represent the power balance at each node of the system, where $\Delta\theta_{(i,j),t,\xi}$ are decision variables associated to the voltage angles differences between nodes i and j at period t for scenario ξ and $B_{(i,j)}$ (Ω^{-1}) is the subsceptance of line $(i,j)\in\mathcal{L}$. In (12) and (13), the power output of a conventional generation unit g is correspondingly limited by its technical minimum and maximum capacity, i.e., $P_g^{\min}$ and $P_g^{\max}$ (MW). Constraints set (13) also considers the decision variables $r_{g,t,\xi} \ge 0$ (MW) defining the spinning reserve for generation unit g at period t for scenario ξ. The systemic spinning reserve requirement at period t is established by $r_t^{\min}$ (MW), whose satisfaction is ensured by (14). Constraints set (15) defines the power balance for a wind power generator g, i.e., the sum of its power output $P_{g,t,\xi}$ and curtailment $PC^{\mathrm{W}}_{g,t,\xi}$ equals the available wind power at period t for scenario ξ. It must be pointed out that $PC^{\mathrm{W}}_{g,t,\xi} \ge 0$ (MW) are decision variables. The capacity of transmission lines $P^{\mathrm{R}}_{(i,j)}$ (MW) is imposed by constraints sets (16) and (17). On the other hand, constraints sets (18) and (19) limit the upward and downward ramping capacities of a conventional generation unit g by the corresponding ramp rates r_g^{U} and r_g^{D} (%), defined as a percentage of its maximum capacity, or by start up and shut down ramp rates, r_g^{SU} and r_g^{SD} (MW), when g has been started up or shut down at period t. Constraints sets (20) and (21) ensure the estimation of the excluding positive or negative power out ramp provided by generation unit g from period $t-1$ to t for the scenario ξ, for evaluating the associated ramping costs.

It is worth mentioning that, in this work, we consider the DC power flow assumptions (i.e., lossless transmission lines, flat voltage profile and small voltage angles differences) will hold with an acceptable error, even during peak load, for systems whose transmission lines X/R are above 5 and present a mesh topology, as suggested by [11] and [12]. Moreover,

E. Method of solution

The proposed two-stage stochastic UC optimization model has been formulated as a MILP and solved directly by a traditional exact method, specifically, a linear programming-based branch and bound algorithm.

III. Flexibility assessment

In this work, a generation-side flexibility assessment is made *a posteriori*, once the optimal on/off schedule has been determined. This assessment is based on the comparison of quantities representing the net flexibility requirements, imposed by the net-load, and the available flexibility in the system, and can shed valuable insights for analyzing the occurrence of events for which amounts of energy not supplied or wind power curtailment arise due to flexibility insufficiency.

Considering the above, the net-flexibility requirement NFR (MW), for one time step $(t,t+1)$, with $t\in\mathcal{T}, t\le|\mathcal{T}|-1$, and for a given scenario $\xi\in\Omega$, can be defined as the aggregated deployment of power needed from the conventional generation fleet, from period t to $t+1$, to meet the net-load at $t+1$, as expressed in (22):

$$NFR_{(t,t+1),\xi} = ND_{t+1,\xi} - \sum_{g\in\mathcal{G}} P_{g,t,\xi} \quad (22)$$

where ND (MW) is the net-load defined in (23) as the total demand-less available wind power at period $t\in\mathcal{T}$ for scenario $\xi\in\Omega$:

$$ND_{t,\xi} = \sum_{i \in \mathcal{N}} D_{i,t,\xi} - \sum_{i \in \mathcal{N}} \sum_{g \in \mathcal{W}_i} P^{\mathrm{W}}(ws_{i,t,\xi}) \quad (23)$$

It is important to note that net-flexibility requirements $NFR_{(t,t+1),\xi}$ can be for an upward (≥ 0) or downward(≤ 0) of power deployment.

On the other hand, the available flexibility at period t measures the aggregated power that can be effectively deployed by the conventional generation fleet to period $t+1$, to meet the net-load at $t+1$. For each conventional generator in the system, this deployment is conditioned by its capability of cycling and ramping over time, attributes which are represented in the proposed UC model. Then, the available upward and downward flexibility, $F^{\mathrm{U}}_{g,(t,t+1),\xi}$ and $F^{\mathrm{D}}_{g,(t,t+1),\xi}$, for a conventional generation unit $g \in \mathcal{G}$ for one time step $(t, t+1)$, with $t \in \mathcal{T}, t \leq |\mathcal{T}| - 1$, and scenario $\xi \in \Omega$, are respectively defined as:

$$F^{\mathrm{U}}_{g,(t,t+1),\xi} = \min\{r^{\mathrm{U}}_g P^{\max}_g, P^{\max}_g - P_{g,t,\xi}\} x_{g,t} x_{g,t+1} + r^{\mathrm{SU}}_g (1 - x_{g,t}) x_{g,t+1}, \quad (24)$$

$$F^{\mathrm{D}}_{g,(t,t+1),\xi} = -\min\{r^{\mathrm{D}}_g P^{\max}_g, P_{g,t,\xi} - P^{\min}_g\} x_{g,t} x_{g,t+1} - r^{\mathrm{SU}}_g (1 - x_{g,t+1}) x_{g,t}, \quad (25)$$

The available upward and downward flexibility in the system, $F^{\mathrm{U}}_{g,(t,t+1),\xi}$ and $F^{\mathrm{D}}_{g,(t,t+1),\xi}$, for one time step $(t, t+1)$ correspond to the summation over the set of conventional generation units $\mathcal{G}$, and attend correspondingly upward and downward net-flexibility requirements $NFR_{(t,t+1),\xi}$. Then, the (in)sufficiency of flexibility to accommodate variable wind power over time can be measured by the net-deficit of flexibility metric NDF proposed by [7], here properly adapted to the proposed methodology. Thus, the net-deficit of flexibility $NDF_{(t,t+1),\xi}$ for one time step $(t, t+1)$, with $t \in \mathcal{T}, t \leq |\mathcal{T}| - 1$, and scenario $\xi \in \Omega$, is defined as follows:

$$NDF_{(t,t+1),\xi} = \begin{cases} NFR_{(t,t+1),\xi} - \sum_{g \in G} F^{\mathrm{U}}_{g,(t,t+1),\xi} & * \\ \sum_{g \in G} F^{\mathrm{D}}_{g,(t,t+1),\xi} - NFR_{(t,t+1),\xi} & ** \end{cases} \quad (26)$$

where, $*$ and $**$ stand for conditions $NFR_{(t,t+1),\xi} \geq 0$ and $NFR_{(t,t+1),\xi} \leq 0$, respectively.

In this way, for a given optimal on/off schedule defining the status variables $x_{g,t}$ for each conventional generator $g \in \mathcal{G}$ and the corresponding power outputs $P_{g,t,\xi}$, it is possible to observe and analyze, for a given scenario $\xi \in \Omega$ and time step $(t, t+1)$, non-negative and non-positive occurrences of $NDF_{(t,t+1),\xi}$, implying insufficiency and sufficiency of flexibility to meet the requirements imposed by the net-load.

IV. Application

The implementation of the proposed two-stage stochastic UC model and *a posteriori* flexibility assessment is performed on a modification of the New England IEEE 39-Bus test system [13], [14], which is described in the following.

A. System description

The determination of the optimal on/off schedule is performed for an horizon of $|\mathcal{T}| = 24$ (h) with hourly resolution, i.e., $\Delta t = 1$ (h). The system under consideration presents $|\mathcal{G}| = 10$ conventional generation units. The aggregated maximum generation capacity in the system is 7367 (MW). In addition, the system has $|\mathcal{L}| = 46$ lines, whose technical parameters, i.e., capacity $P^{\mathrm{R}}_{(i,j)}$ (MW) and subsceptance $B_{(i,j)}$ (Ω^{-1}), $\forall (i,j) \in \mathcal{L}$, are obtained from [14]. A diagram of the New England IEEE 39-Bus test system can be found in [15].

The type of technology, technical and cost parameters of the conventional power generation units are reported in Tables I and II. Start up and shut down ramp rates, r^{SU}_g and r^{SD}_g (MW), are set equal to $P^{\min}_g$ (MW), and the shut down cost C^{SD} (US$) is considered negligible [13].

TABLE I
Location, type and technical parameters of conventional power generation units [13], [14], [16], [17].

Node	Tech.	H_g	μ^{f}_g	$P^{\max}_g$	$P^{\min}_g$	$r^{\mathrm{U}}_g, r^{\mathrm{D}}_g$	$t^{\mathrm{U}}_g, t^{\mathrm{D}}_g$
i		[a]	[b]	(MW)	(MW)	(%)	(h)
30	Hydro	-	-	1040	624	1.00	5
31	Coal	10.65	0.103	646	207	0.15	2
32	Gas	7.81	0.053	725	327	0.30	2
33	Coal	10.65	0.103	652	209	0.15	2
34	Gas	7.81	0.053	508	229	0.30	2
35	Coal	10.65	0.103	687	220	0.15	2
36	Gas	10.83	0.073	580	290	0.50	1
37	Coal	10.65	0.103	564	180	0.15	2
38	Nuke	10.46	-	865	346	0.05	5
39	I.C.[c]	8.00	0.100	1100	440	0.10	1

[a] in (MMBtu/MWh).
[b] in (MtonCO_2/MMBtu).
[c] Interconnection.

TABLE II
Location and cost parameters of conventional power generation units [13], [17].

Node	C^{OM}_g	C^{F}_g	C^{SU}_g	C^{R}_g
i	(US$/MWh)	(US$/h)	(kUS$/h)	(US$/$\Delta$MW)
30	9.19	1000	-	-
31	17.55	680	43.09	2.233
32	21.80	450	21.45	1.471
33	16.50	680	43.49	2.213
34	19.70	450	15.03	1.600
35	16.50	680	45.82	2.100
36	27.74	480	20.18	1.839
37	20.10	680	37.62	2.558
38	23.11	1200	24.08	-
39	21.79	670	18.63	1.452

The mean μ_t and standard deviation values σ_t, $\forall t \in \mathcal{T}$, of the hourly normally distributed aggregated daily demand profile are reported in Table III [13]. The nodal factors $p_i, \forall i \in \mathcal{N}$, to weigh down a sampled aggregated demand profile and determined nodal profiles, are derived from [14].

In regards to wind power generation, to accentuate the effects of wind power variability in the system, all wind power capacity is arbitrarily concentrated at node 6. The wind farm

TABLE III
MEAN AND STANDARD DEVIATION OF THE HOURLY AGGREGATED DEMAND PROFILE [13], [17].

$t \in \mathcal{T}$	μ_t (MW)	σ_t (MW)	$t \in \mathcal{T}$	μ_t (MW)	σ_t (MW)
1	2139.12	267.39	13	4278.25	534.78
2	2291.92	286.49	14	3972.66	496.58
3	2597.51	324.69	15	3667.07	458.38
4	2903.10	362.89	16	3208.68	401.09
5	3055.89	381.99	17	3055.89	381.99
6	3361.48	420.18	18	3361.48	420.18
7	3514.27	439.28	19	3667.07	458.38
8	3667.07	458.38	20	4278.25	534.78
9	3972.66	496.58	21	3972.66	496.58
10	4278.25	534.78	22	3361.48	420.18
11	4431.04	553.88	23	2750.30	343.79
12	4583.84	572.98	24	2444.71	305.59

subscribes a rated capacity of 2000 (MW), corresponding to $N_i^{\mathrm{W}} = 1000$ wind turbines with rated power $P^{\mathrm{W}} = 2$ (MW), based on the Vestas V90 technology. Consequently, the cut-in, rated and cut-out wind speed for the wind energy conversion model in (1) are $U^{\mathrm{in}} = 4$, $U^{\mathrm{R}} = 13$ and $U^{\mathrm{out}} = 25$ (m/s), respectively. To model wind speed at node 6, a SARIMA model is fitted to an annual wind speed time series with hourly resolution. This wind speed time series is obtained from [18], and presents a Weibull-like distribution with approximated shape and scale parameters $k = 2$ and $a = 7$, respectively, implying an annual average wind speed of 6.2 (m/s).

Additional parameters set for calculation of the objective function include the carbon cost $C^{\mathrm{CO_2}} = 5$ (US$/MtonCO$_2$) and the penalty for energy not supplied $C_i^{\mathrm{ENS}} = 9000$ (US$/MWh), $\forall i \in \mathcal{N}$. It is important to mention that the variable O&M generation cost C_g^{OM} for wind power is regarded as 0 (US$/MWh), which is a common assumption found in the literature.

A set of $|\Omega| = 100$ of 24 (h) length discrete time series for the aggregated demand and wind speed at node 6 were considered as inputs for the proposed MILP two-stage stochastic UC model. The model was implemented in Python, by means of the package Pyomo, and run on an Intel I7 processor with 2.70 GHz and 16 Gb of RAM. Gurobi 9.1.1. was set as solver.

B. Results

The obtained cost-optimal on/off schedule presented in Fig. 1 is coherent with the mean profile of the aggregated demand, i.e., more conventional generators g are in on status ($x_{g,t} = 1, \forall g \in \mathcal{G}, t \in \mathcal{T}$ (white cells) around peak hours, and in off status $x_{g,t} = 0$ (black cells) during low demand hours. It can be noticed that the optimal schedule relies mostly on coal, gas and hydro technologies, in a effort to balance cycling and ramping cost and penalties for incurring in energy not supplied vs. the carbon cost and the negligible variable O&M cost associated to wind power generation.

The optimal on/off schedule subscribes a total expected cost of approx. 4.043 (MUS$), with a level of expected CO_2 emissions of 41.124 (Mton), expected energy not supplied of 152.7 (MWh) and expected percentage of wind power curtailment of 23 (%). Even though the obtained on/off schedule provides a cost-effective performance, the rate of wind power curtailment

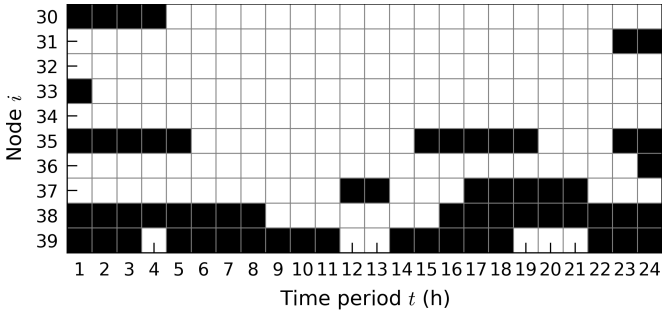

Fig. 1. Optimal on/off schedule.

suggests a less adequate performance concerning flexibility. To analyze this, we refer to the quantities used to measure flexibility performance for the operational scenario $\xi = 7$. This scenario can be considered extreme since it presents a high level of wind power available of approx. 36485 (MW), with an approximate 36 (%) of curtailment. Figs. 2 and 3 show the aggregated power dispatching by generation technology and the flexibility assessment quantities for scenario $\xi = 7$, respectively.

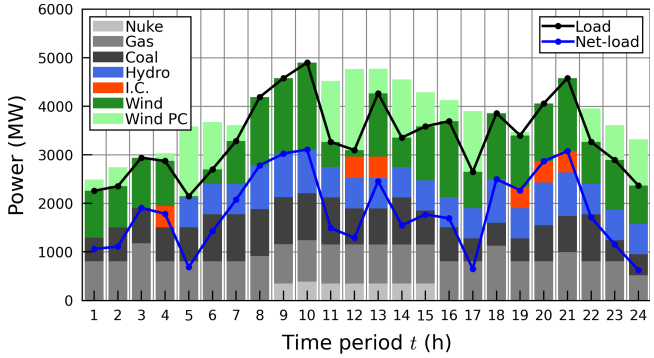

Fig. 2. Aggregated power dispatching by generation technology. Scenario $\xi = 7$.

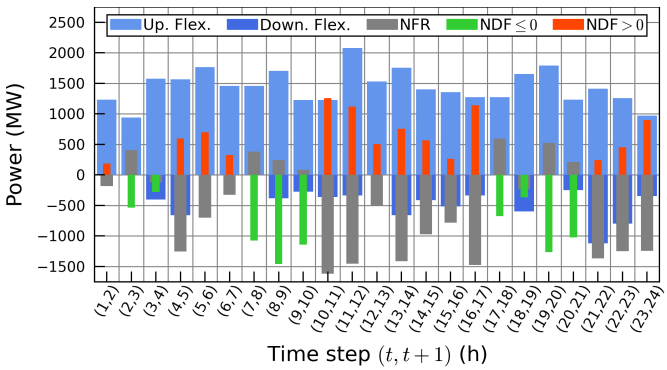

Fig. 3. Flexibility assessment quantities. Scenario $\xi = 7$.

As it can be observed in Fig. 2, given the cost-optimal on/off schedule and the dispatching decisions for scenario $\xi = 7$, the aggregated power output of conventional generation units does not match the net-load throughout all periods $t \in \mathcal{T}$. This translates into upward and downward NFR values for

some time steps $(t, t+1)$ within $\mathcal{T}$, as shown in Fig. 3. Moreover, considering that at the dispatching decisions level, avoiding energy not supplied is prioritized over wind power curtailment, the observed amounts of this latter quantity in Fig. 2 (Wind PC) are mostly attributed to the scheduling decisions. For instance, the postponement of the start up of the coal-based and hydro units from periods 2 to 3 and 5 to 7, would have served to decrease wind power curtailment.

To complement the above-mentioned findings, Fig. 3 presents an imbalance between available upward and downward flexibility. In fact, most observations of deficit, i.e., $NDF > 0$, are due to insufficient downward flexibility, limited mainly by the restricted cycling provided by the cost-optimal on/off schedule. In other words, the cost-based UC model decides not to frequently start up and shut down generation units to avoid incurring in cycling costs. This is noticeable in Figs. 1 and 2, from the behavior of the gas-based units and interconnection at nodes 36 and 39, respectively, both presenting the lower cool down and warm up times. The frequent cycling of these type of units would provide more available downward flexibility to accommodate more wind power, especially, for time steps $(t, t+1)$ with downward NFR.

Then, a valid research question that can be formulated regarding the integration of flexibility assessment quantities into the commitment decision-making process to design on/off schedules that effectively control extreme scenarios with high rates of wind power curtailment, control that is hindered by a pure cost-based criteria.

V. Conclusions

This work has presented a two-stage stochastic unit commitment model to determine a cost-optimal on/off schedule for a wind-integrated power system. The proposed model accounts for uncertainty in wind power generation and the aggregated demand of the system. A sequential MCS is performed to sample a set of realizations of these uncertain parameters within the time horizon of analysis.

An ex-post flexibility assessment is integrated into the modeling framework to analyze how adequate are the cost-based scheduling decisions to cope with the occurrence of extreme scenarios with considerable amounts of wind power curtailment.

An application of the proposed model is performed on a modification of the New England IEEE 39-Bus system. The results show the capability of the modeling framework in building a cost-efficient on/off schedule and providing useful insights to study the operational behavior of the system, confronting undesired operational outcomes with the sufficiency or insufficiency of flexibility.

Future work will address the challenge of integrating flexibility quantities into the decision-making process, for designing on/off schedules that trade-off operational cost and the extent of provided and used flexibility, to accommodate higher rates of variable wind power, without compromising the reliability of power supply.

References

[1] Y. Chang, Z. Fang, and Y. Li, "Renewable energy policies in promoting financing and investment among the east asia summit countries: Quantitative assessment and policy implications," *Energy Policy*, vol. 95, pp. 427–436, 2016. [Online]. Available: https://www.sciencedirect.com/science/article/pii/S0301421516300581

[2] International Energy Agency (IEA), "World energy outlook 2020." [Online]. Available: https://www.iea.org/reports/world-energy-outlook-2020

[3] B. Zhou, J. Fang, X. Ai, W. Yao, and J. Wen, "Flexibility-enhanced continuous-time scheduling of power system under wind uncertainties," *IEEE Transactions on Sustainable Energy*, vol. 12, no. 4, pp. 2306–2320, 2021.

[4] Y. Zhao, C. Wang, Z. Zhang, and H. Lv, "Flexibility evaluation method of power system considering the impact of multi-energy coupling," in *2021 IEEE/IAS 57th Industrial and Commercial Power Systems Technical Conference (I CPS)*, 2021, pp. 1–10.

[5] E. Zio, "Challenges in the vulnerability and risk analysis of critical infrastructures," *Reliability Engineering & System Safety*, vol. 152, pp. 137 – 150, 2016. [Online]. Available: http://www.sciencedirect.com/science/article/pii/S0951832016000508

[6] H. Berahmandpour, S. M. Kouhsari, and H. Rastegar, "A new flexibility index in real time operation incorporating wind farms," in *2019 27th Iranian Conference on Electrical Engineering (ICEE)*, 2019, pp. 549–553.

[7] E. Lannoye, P. Daly, A. Tuohy, D. Flynn, and M. O'Malley, "Assessing power system flexibility for variable renewable integration: A flexibility metric for long-term system planning," *CIGRE Science and Engineering Journal*, vol. 3, pp. 26–39, 2015.

[8] A. Hajebrahimi, A. Abdollahi, and M. Rashidinejad, "Probabilistic multiobjective transmission expansion planning incorporating demand response resources and large-scale distant wind farms," *IEEE Systems Journal*, vol. 11, no. 2, pp. 1170–1181, 2017.

[9] J. L. Tena García, E. Cadenas Calderón, G. González Ávalos, E. Rangel Heras, and A. Mbikayi Tshikala, "Forecast of daily output energy of wind turbine using sarima and nonlinear autoregressive models," *Advances in Mechanical Engineering*, vol. 11, no. 2, p. 1687814018813464, 2019.

[10] R. Ma and G. M. Huang, "Impact analysis of wind generation on voltage stability and system load margin," in *Proceedings of the 2011 American Control Conference*. IEEE, 2011, pp. 4166–4171.

[11] K. Purchala, L. Meeus, D. Van Dommelen, and R. Belmans, "Usefulness of dc power flow for active power flow analysis," in *IEEE Power Engineering Society General Meeting, 2005*, June 2005, pp. 454–459 Vol. 1.

[12] K. Van den Bergh, E. Delarue, and W. D'haeseleer, "Dc power flow in unit commitment models," *no. May*, 2014.

[13] G. Yehescale and M. D. Reddy, "A new strategy for solving unit commitment problem by pso algorithm," in *2018 IEEE International Conference on Current Trends in Advanced Computing (ICCTAC)*. IEEE, 2018, pp. 1–6.

[14] MatPower, "Case39 power flow data for 39 bus new england system." 2014, [Last access november 2019].

[15] Texas A&M University's energy and power group, "Electric grid test case repository," 2016. [Online]. Available: https://electricgrids.engr.tamu.edu/electric-grid-test-cases/ieee-39-bus-system/

[16] U.S. Energy Information Adminstration (EIA) , "Electric power annual 2018," Tech. Rep. October, 2019.

[17] K. Van den Bergh and E. Delarue, "Cycling of conventional power plants: Technical limits and actual costs," *Energy Conversion and Management*, vol. 97, pp. 70–77, 2015. [Online]. Available: https://www.sciencedirect.com/science/article/pii/S0196890415002368

[18] Ministerio De Energía, "Explorador de Energía Eólica," 2014. [Online]. Available: http://walker.dgf.uchile.cl/Explorador/Eolico2/